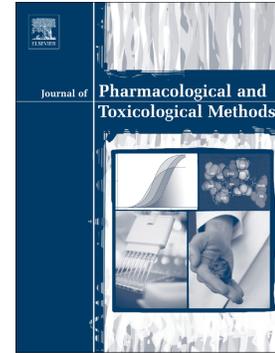# Accepted Manuscript

Measuring kinetics and potency of hERG block for CiPA

Monique J. Windley, Najah Abi-Gerges, Bernard Fermini, Jules C. Hancox, Jamie I. Vandenberg, Adam P. Hill

Please cite this article as: Monique J. Windley, Najah Abi-Gerges, Bernard Fermini, Jules C. Hancox, Jamie I. Vandenberg, Adam P. Hill , Measuring kinetics and potency of hERG block for CiPA. The address for the corresponding author was captured as affiliation for all authors. Please check if appropriate. Jpm(2017), doi: 10.1016/j.vascn.2017.02.017

Measuring kinetics and potency of hERG block for CiPA

Monique J. Windley[a,b], Najah Abi-Gerges[c], Bernard Fermini[d], Jules C. Hancox[e], Jamie I. Vandenberg[a,b], Adam P. Hill[a,b]

a. Molecular Cardiology and Biophysics Division, Victor Chang Cardiac Research Institute, 405 Liverpool Street, Sydney, NSW 2010, Australia.

b. St. Vincent's Clinical School, University of New South Wales, Sydney, NSW 2052, Australia

c. AnaBios Corp., 3030 Bunker Hill St., San Diego, CA 92109, USA

d. Global Safety Pharmacology, Pfizer Inc., MS8274-1347 Eastern Point Road, Groton, CT 06340, USA

e. School of Physiology, Pharmacology and Neuroscience, University of Bristol, UK

Corresponding Author:

Adam Hill

Computational Cardiology Research Group,

Victor Chang Cardiac Research Institute,

405, Liverpool Street

Darlinghurst,

NSW 2010

Australia

E: a.hill@victorchang.edu.au

T: +61 (0)2 9295 8686

F: +61 (0)2 9295 8770

Abstract

Introduction

The Comprehensive *in vitro* Proarrhythmic assay (CiPA) aims to update current cardiac safety testing to better evaluate arrhythmic risk. A central theme of CiPA is the use of *in silico* approaches to risk prediction incorporating models of drug binding to hERG. To parameterize these models, accurate *in vitro* measurement of potency and kinetics of block is required. The Ion Channel Working Group was tasked with: i) selecting a protocol that could measure kinetics of block and was easily implementable on automated platforms for future rollout in industry and ii) acquiring a reference dataset using the standardized protocol.

Methods

Data were acquired using a 'step depolarisation' protocol using manual patch-clamp at ambient temperature.

Results

Potency, kinetics and trapping characteristics of hERG block for the CiPA training panel of twelve drugs were measured. Timecourse of block and trapping characteristics could be reliably measured if the time constant for onset of block was between ~500 ms and ~15 sec. Seven drugs, however had time courses of block faster than this cut-off.

Discussion

Here we describe the implementation of the standardized protocol for measurement of kinetics and potency of hERG block for CiPA. The results highlight the challenges in identifying a single protocol to measure hERG block over a range of kinetics. The dataset from this study is being used by the *In Silico* Working Group to develop models of drug binding for risk prediction and is freely available as a 'gold standard' ambient temperature dataset to evaluate variability across high throughput platforms.

1. Introduction

Acquired, or drug-induced, long QT syndrome (aLQTS) occurs most often as a result of pharmacological block of hERG (human ether-a-go-go related gene)/Kv11.1 potassium channels in the heart. Reduced hERG function prolongs the QT interval on the surface electrocardiogram and increases the risk of the potentially fatal cardiac arrhythmia torsade de pointes (TdP) (Roden, 2004). Over the past twenty years a range of structurally unrelated cardiac and non-cardiac drugs have been withdrawn from market as a result of these side effects (Shah, 2008). The introduction, in 2005, of a series of mandated tests (ICH S7B and E14) for all new drugs to assess hERG block, cardiac action potential prolongation and QT interval prolongation has meant that no new drugs have been removed from market due to unacceptable Torsadogenic risk in the last decade.

However, eliminating hERG blocking properties from drugs in development is a difficult task since it has been estimated that between 70 and 86% of compounds block hERG at some concentration (Shah, 2008). Furthermore, there is growing concern that whilst current tests are very sensitive, they are not specific, meaning potentially safe drugs are having their development prematurely terminated (Fermini *et al.*, 2016; Gintant *et al.*, 2016; Sager *et al.*, 2014). For example, verapamil has been prescribed to millions of patients worldwide over 40 years with no incidence of TdP despite blocking hERG in its therapeutic range. This apparent anomaly can be explained by verapamil's multichannel pharmacological profile whereby in addition to hERG, it also blocks calcium channels, so ameliorating risk by eliminating early after depolarisation (EAD) triggers for initiation of arrhythmia (Aiba *et al.*, 2005). However, under current preclinical guidelines based on block of hERG channels, verapamil would never have been developed as a therapeutic. It should be noted however, that while it is

impossible to know how many 'safe' compounds in preclinical development have had their development terminated based on positive hERG hits, there are relatively few example of on-market drugs (such as verapamil) where this is the case. Nevertheless, issues such as this have prompted a rethink of how drugs should be tested and have led to the recent proposal of the Comprehensive *in vitro* Proarrhythmic Assay (CiPA) (Fermini *et al.*, 2016; Gintant *et al.*, 2016; Sager *et al.*, 2014). CiPA aims to develop new mechanism based testing that employs actual markers of proarrhythmic propensity as opposed to the relatively poor surrogates (hERG block, AP prolongation) that are currently used to predict this risk. One of the proposed streams of CiPA is the use of *in silico* models of human cardiac electrophysiology incorporating temperature-dependent models of hERG gating (Li *et al.*, 2016) as well as descriptions of drug binding to hERG (and potentially other ion channels), including the kinetics of drug interactions. This approach will allow integration of how drugs with potentially complex state dependent binding kinetics interact with the hERG channel in a dynamic manner during the cardiac action potential to modify repolarisation and risk.

The goal in regard to the practical implementation of the *in silico* aspect of CiPA is that a selected voltage-clamp protocol will be run as part of preclinical development to measure drug binding kinetics to hERG. The data from this protocol will be used to constrain standardized *in silico* models of drug binding to hERG to predict proarrhythmic risk when incorporated into human action potential simulations. To achieve this, the protocol should ideally be able to measure both potency and kinetics of drug binding to hERG and be amenable to data acquisition in the high throughput automated patch clamp systems that are currently employed within industry. To this end, the Ion Channel Working Group (ICWG) and *In Silico* Working Groups (ISWG) identified the step depolarisation protocol described by Milnes *et al.* (Milnes *et al.*, 2010) as a suitable protocol for testing (see Colatsky *et al.*,

2016 for details on the motivation and makeup of the individual working groups within CiPA).

In this study we present the 'gold standard' CiPA dataset describing block of hERG channels by a training panel of 12 drugs, split equally between low, medium and high risk (Colatsky *et al.*, 2016). The data was acquired using manual patch clamp to provide the highest fidelity of recordings and accuracy of measurement against which other automated high throughout approaches can be measured (Hancox *et al.*, 2008). Data was gathered at ambient temperature since this is most relevant to most high throughput platforms on which the assay will be run. In addition to potency of block, we measured the kinetics of onset of block and the extent of drug trapping (the degree to which a drug is able to dissociate from the closed state) using the step depolarisation protocol (Milnes *et al.*, 2010). We observed a much wider variety of kinetics of drug binding than expected. For drugs with kinetics of block that were very slow, we had to extend the duration of the protocol to enable estimation of kinetics of block. Furthermore, we also found that for about half of the drugs tested, the onset of block was at least as fast as the rate of channel activation and so it was not possible to measure the kinetics of binding using the step depolarisation protocol under the recording conditions used in this study. The dataset gathered as part of this study is being used by the *In Silico* Working Group to develop models of drug binding for risk prediction, to evaluate the temperature dependence of drug binding to hERG and is freely available as a 'gold standard' ambient temperature dataset to evaluate variability in automated patch clamp platforms.

2. Materials and methods

2.1 Cell culture

CHO cells stably expressing hERG/K_v11.1 were purchased from the American Type Culture Collection (ATCC reference PTA-6812). Cells were cultured in Hams F12 nutrient mix (ThermoFisher Scientific, Waltham, USA) containing 5% fetal bovine serum (Sigma-Aldrich, Sydney, Australia) and maintained at 37 ^{0}C with 5% CO_2.

2.2 Patch clamp

Whole cell patch clamp currents were evoked from CHO cells in the voltage clamp configuration at 22^{0}C. The current signal was amplified and filtered at 1 kHz with an Axopatch 200B (Molecular Devices, Sunnyvale, USA) and sampled at 5 kHz with a PC interfaced with an analog to digital converter, Digidata1440A (Molecular Devices). Series resistance compensation was >80%. Leak currents were subtracted manually offline. Data was acquired with pCLAMP 10 (Molecular Devices) acquisition software and analysed using Clampfit (Molecular Devices) and Prism (v6, GraphPad, San Diego, USA).

Single use patch pipettes were pulled from borosilicate glass (Harvard Apparatus, Holliston, USA) with resistances of 2-5 MΩ. Pipettes were filled with internal solution containing (in mM): 120 potassium gluconate, 20 KCl, 1.5 Mg_2ATP, 5 EGTA and 10 HEPES, adjusted to pH 7.2 with KOH. The external bath solution contained (in mM); 130 NaCl, 5 KCl, 1 $MgCl_2$, 1 $CaCl_2$, 12.5 glucose and 10 HEPES, adjusted to pH 7.4 with NaOH. The calculated liquid junction potential of -15 mV (Barry, 1994) was corrected for by adjusting voltage pulse protocols prior to stimulation. For the experiments presented in this paper the whole cell seal resistance was 1.6 +/- 0.1 GΩ, access resistance was 4.6 +/- 0.2 MΩ, holding current was -

21.1 +/- 1.4pA and cell capacitance was 20.5 +/- 0.5 pF (n = 138, mean +/- SE) (see Supplementary Figure S1)

2.3 Drug application/Pharmacology

The CiPA Clinical Translation Working Group (CTWG), an expert team of cardiac electrophysiologists, safety pharmacologists and clinicians, selected a panel of 12 drugs split equally between low, intermediate and high proarrhythmic risk, on which *in vitro* testing against hERG channels would be centred (Table 1) (Colatsky *et al.*, 2016). The concentrations selected for testing were based on previously published data (Antzelevitch *et al.*, 2004; Crumb *et al.*, 2016; Gualdani *et al.*, 2015; Redfern *et al.*, 2003), albeit gathered under different conditions and protocols. The fold difference from the maximum free plasma concentration (Free C_{max}) (Crumb *et al.*, 2016) is also listed in Table 1.

The Dynaflow Resolve (Cellectricon, Mölndal, Sweden) microfluidic solution exchange system was used to apply drugs (solution exchange time <30 msHill *et al.*, 2014). Where necessary for solubility, drugs were dissolved in DMSO. The maximum amount of DMSO never exceeded 0.1% (v/v), a concentration which has been shown to have no effect on hERG channel activity (Walker *et al.*, 1999).

2.4 Data analysis

Steady state concentration-response data were fit with the Hill equation:

$$y = \frac{1}{1+([x]/IC_{50})^{n_H}}$$

Eqn 1

where [x] is drug concentration, n_H is the Hill coefficient (slope parameter), and IC_{50} is the concentration at which 50% block of channel current is evident. For simplicity, the Hill curves fit to the concentration response data were constrained to minima of 0 and maxima of 100 % block.

To measure the kinetics of drug block, the timecourse of the block onset was calculated through offline subtraction:

$$\% \, block = \left(\frac{i-ii}{i}\right) \times 100 \qquad \text{Eqn 2}$$

Where i is the control current trace (no drug) and ii is the first trace in the presence of drug. The percentage block data was fitted with a standard exponential function yielding a single time constant (τ_{on}):

$$f(t)_{on} = (I_m - I_d) \times \left(e^{-t/\tau_{on}}\right) + I_d \qquad \text{Eqn 3}$$

Where I_m is the maximum percentage block at t = 0, I_d is the percentage block plateau amplitude in the presence of drug, t is time, τ_{on} is the time constant.

2.5   Chemical compounds

All chemicals were supplied by Sigma-Aldrich (Sydney, Australia) unless otherwise stated.

3. Results

3.1 Protocol implementation

The step depolarisation protocol from Milnes *et al.* (Milnes *et al.*, 2010) was chosen by the ICWG and ISWG as the standard protocol for gathering data describing kinetics of drug binding to hERG for CiPA (Figure 1). The basic protocol unit has a 25 s start-to-start time including a 10 s depolarizing step to 0mV with a 15 s interpulse interval at a holding potential of -80 mV (Figure 1Ai). For data acquisition, the protocol was run in three phases (Figure 1). Initially the 0 mV 10s voltage pulse was repeated 5 times in the absence of drug to ensure currents were stable and to obtain control current profiles (sweeps 1-5, Figure 1Ai). Following this a further 5 sweeps, without the depolarizing step, where the cell membrane was held at -80 mV for 25s each (total 125 s) were acquired while the drug is washed into the system (sweeps 6-10, Figure 1Aii) with the channel closed. Finally, a third phase of five sweeps of the basic protocol including the depolarizing step to 0 mV were acquired, in the continued presence of drug during which the onset of block is visible as the reduction in the hERG current over the duration of the 10 s depolarizing step (sweeps 11-15, Figure 1Aiii). In this example, the drug block reached equilibrium within the first sweep, meaning subsequent current traces are directly overlaid. The percentage of drug block measured at the end of the 5th drug sweep (sweep 15, Figure 1Aiii) was used to measure the potency of the drug and to plot concentration response curves (see for example Figure 3).

To measure the kinetics of the onset of drug block the hERG currents were subtracted offline and fit with exponential curves. Specifically, the first hERG current trace recorded in response to the 0 mV voltage step in the presence of drug (sweep 11, (ii) Figure 1B, left) was subtracted from the last hERG trace before drug was perfused (sweep 5, (i) Figure 1B, left). The percentage block over time was then calculated by dividing the subtracted trace by the

last control trace (sweep 5) and multiplying by 100 (Figure 1B, right). An exponential function was fit to the percentage block data to give a single time constant representing the timecourse of drug block (see Materials and Methods).

3.2 Potency of hERG block

All of the drugs tested, with the exception of dofetilide, had at least one concentration that reached steady state block within or close to the end of the first 10 s voltage pulse. Representative raw hERG current traces recorded in response to ~IC_{50} concentrations, for those drugs where the 10 s pulse was sufficient for all 3 concentrations tested to reach steady state are shown in Figure 2. The concentration response curves for all 12 drugs are plotted in figure 3. The IC_{50} values, together with a comparison to previously published data, are listed in Table 2.

3.3 Kinetics of hERG block

Measured time constants for the onset of drug block (τ_{on}) for the eleven drugs where the timecourse of block could be reliably measured for at least one concentration using the standard 10 s protocol are shown in Figure 4. For some drugs (cisapride and verapamil), a clear concentration dependence for the timecourse of block onset is observed using this initial implementation of the protocol. For example, τ_{on} was measured as 5.6 ± 0.6 s, 3.1 ± 0.3 s and 1.9 ± 0.2 s for 100, 300 and 1000 nM verapamil, respectively. However, for those drugs with faster kinetics (quinidine, sotalol, chlorpromazine, diltiazem, mexiletine, onsansetron and ranolazine), no concentration dependence of the time course of onset of block was apparent but rather some block appeared as an instantaneous effect that was present as soon as the channel opened. We considered that this could potentially be explained by one of two reasons: first, for these drugs the onset of block was faster than the rate of hERG channel

activation at 0 mV and therefore could not be accurately resolved using this protocol; or second, that the drug was able to block the channel in the closed state during the drug equilibration period at -80 mV (sweeps 6-10, Figure 1Aii). To address this question we used the Dynaflow resolve microfluidic solution exchange system (Cellectricon, Sweden) to directly measure the timecourse of onset of block at 0 mV for a subset of the drug panel. A typical example showing block and washoff profiles for 10, 30 and 100 μM diltiazem is shown in Figure 5B. To analyse data gathered using this protocol, an exponential function was directly fitted to the timecourse of current decay during application of drug to measure the timecourse of block (Figure 5D) (Hill *et al.*, 2014). In contrast to the step depolarisation protocol, a clear concentration dependence of the timecourse for onset of block for fast drugs could be resolved using this approach with τ_{on} values measured as 299 ± 42, 204 ± 38 and 114 ± 34 ms for 10, 30 and 100 μM diltiazem respectively (mean ± SE, n = 4-5, Figure 5E). Similar results were observed for other fast drugs tested (ranolazine and mexiletine, Supplementary Figure 3) providing evidence that these drugs do block as fast, or faster than the rate of channel opening at 0 mV hence the inability to obtain accurate measurements of the timecourse of the onset of block using the step depolarisation protocol.

A second limitation of the initial implementation of the protocol (that incorporated the 10 s depolarizing step) was the inability to measure kinetics of block for those drugs where the timecourse of the onset of block was very slow. Specifically, low concentrations of cisapride, bepridil and terfenadine as well as all concentrations of dofetilide did not reach steady state block within the 10 s time period (Figure 6A) and yielded highly variable results when fit with an exponential curve. To examine this in more detail, we analysed the measured timecourse of the onset of block for 30 nM cisapride as a function of the duration of the depolarizing pulse (Figure 6B). While no reliable fit could be obtained with a 10 s

depolarizing step, we saw a large standard error when measurements were made with a 20 s step (206 ± 393 s), that was reduced with a 30 s step (31 ± 14 s) and even further at 40 s (26 ± 7 s). As a rule, the step should be 2-3 times the time constant to obtain a consistent measurement. Similar results were seen for other slow drugs (data not shown) and subsequently a modified protocol incorporating a longer 40 s 0mV pulse protocol was introduced for the subset of drugs where 10 s was not sufficient to measure onset of block. Representative traces for each of the 4 drugs used with the 40 s protocol are shown in Figure 6C. While 3 of the 4 drugs reached close to steady state block within the 40 s duration it is evident that for 10 nM dofetilide the length of the protocol was still not sufficient for steady-state inhibition to occur, reaching only 20.7 ± 1.8 % of the final 68.6 ± 8.3% block within the first 40 s sweep (n = 4). The variability in the measured onset of block for 10 nM dofetilide is clearly evident in Figure 6D and kinetic data for 3 nM dofetilide is absent as the degree of block was negligible in the first 40 s sweep. The other τ_{on} values obtained from 40s 0 mV pulses are shown in Figure 6D and combined with other 10 s 0 mV data obtained with the same drugs to further demonstrate the concentration dependency of the block kinetics (see supplementary figure 2 and table 1 for a summary kinetic data for entire drug panel).

3.4 Drug trapping

Another parameter that can be approximated to some degree from this dataset, and may be important in characterising the nature of drug/hERG interactions, was the degree of drug trapping. Trapping refers to the phenomenon that upon closing of a drug-bound channel in response to membrane repolarisation, a drug might be unable to dissociate from the closed state as it is 'trapped' in the channel pore (Mitcheson *et al.*, 2000). As a result of this, upon subsequent depolarisation of the membrane and accompanying activation of the hERG channel, a proportion of the population remains drug bound, depending on the degree of

trapping that has occurred. To determine the extent of drug trapping, we estimated the percentage channel block at the start of the 5th sweep in the presence of drug (sweep 15), as illustrated in Figure 7A. Sweep 15 was fitted with an exponential curve, excluding the first 0.5 s due to the high degree of noise, and this fit was extrapolated back to t = 0. The degree of block at time point 0 was then expressed as a percentage of the block at the end of the 10 or 40 s depolarization step for sweep 15. In the example illustrated in Figure 7A, the extent of block at the start of the 15th sweep was 73% of the block observed at the end of the 15th sweep (see supplementary figure 4 for a summary of trapping for sweeps 12 to 15). The highest concentration of drug tested was used to do this calculation and due to the noise within the first 0.5 s of the trace only drugs with τ_{on} values >500 ms resulted in meaningful measurements. The degree of trapping measured was >90% for two drugs, dofetilide, and terfenadine (98.1, 97.3 and trapped respectively, Figure 7B). In comparison, bepridil and cisapride were 78.7% and 64.7% trapped while verapamil block was almost completely relieved at the beginning of each sweep (only 17.8% trapped).

4. Discussion

In this study we present the 'gold standard' manual patch clamp dataset describing hERG channel block at ambient temperature for the CiPA training panel of twelve drugs. Using a 'step depolarisation' protocol modified from Milnes *et al.* (Milnes *et al.*, 2010) we measured potency, kinetics of onset of block and drug trapping –features that are anticipated will be employed in developing *in silico* models for pro-arrhythmia risk prediction as part of CiPA. Our data showed that for slow drugs, a modification of the initial implementation of the protocol was needed to accurately measure kinetics, while for drugs whose onset of block occurred faster than the rate of channel activation at 0 mV, timecourse of block development could not be fully resolved across all concentrations using this protocol. The methodology described here provides a blueprint for implementation in industry, while the dataset (all raw data openly available along with this publication) serves as a benchmark for assessing variability of future datasets gathered using high throughput automated patch clamp systems, operated at room temperature.

4.1 Protocol selection

Selection of the voltage protocol by the ICWG was based on the requirement to characterise both potency and kinetics of hERG channel block such that the data could be used to constrain models of hERG/drug interaction for use in *in silico* pro-arrhythmia risk prediction (Fermini *et al.*, 2016). Furthermore, the protocol needed to be amenable to implementation in current high throughput automated patch clamp systems, as these are the systems on which the protocol will be run in future drug screening pipelines. The 'step depolarisation' protocol from Milnes *et al* (Milnes *et al.*, 2010) was chosen as a suitable candidate to meet these requirements. The initial implementation of the protocol consisted of three phases: control (Figure 1Ai), drug equilibration (Figure 1Aii) and onset of drug block (Figure 1Aiii). The

rationale of the equilibration phase, during which the membrane potential is held at -80 mV throughout, is that drugs cannot block the channel in the closed state since they cannot reach the binding site located in the pore cavity between the selectivity filter and the cytoplasmic gate (Carmeliet, 1992; Mitcheson *et al.*, 2000; Spector *et al.*, 1996). This phase therefore allows the drug to wash into the system, taking into account solution exchange times as well as equilibration of drug into the cytosol of the cell, without blocking the channel. This ensures that the timecourse measured in the 'drug block' phase reflects only the kinetics of the drug/channel interaction, and not properties of the recording system. In this implementation of the protocol, each phase consisted of five sweeps, based on the original description in Milnes *et al* (Milnes *et al.*, 2010). This approach allowed enough control sweeps to assess stability of the recording, as well as sufficient time for equilibration of drug. However, it is conceivable that for systems with slow solution exchange times for example, more repetitions of the individual phases may be required for equilibration.

4.1.1 Drugs with slow binding kinetics

The initial implementation of the protocol, incorporating a 10 s 0mV step (as originally described in Milnes *et al.*, 2010) was too short to accurately measure the timecourse of the onset of block during a single protocol application for at least one concentration of four of the drugs tested (bepridil, cisapride, terfenadine, dofetilide). As a consequence, we adjusted the protocol to increase the duration of the 0 mV step to 40 s, for slow binding drugs. This modification enabled the accurate measurement of all concentrations of each of the slower blocking drugs, with the exception of dofetilide. For 100 nM dofetilide the degree of block only reached 77% by the end of the first 40 s sweep compared to a final equilibrated block of 97 %. Furthermore, block by 10 nM dofetilide was highly variable and 3 nM dofetilide was indistinguishable from control currents. Based on these observations, we suggest that the step

depolarisation should be run in two stages when employed at room temperature: stage 1, with a 10 s depolarizing step, to assess the broad range of kinetics of the compound being tested; stage 2 (if deemed necessary due to slow kinetics identified in Stage 1) with a 40 s depolarizing step to accurately measure the timecourse of the onset of block.

In previous publications using the step depolarisation protocol at physiological temperature, the onset of block for dofetilide could be accurately measured within the timeframe of the 10 s depolarizing step (τ_{on} = 3 s for 60 nM dofetilide (Milnes *et al.*, 2010). These results suggest that, at least for dofetilide, the kinetics of block are very temperature sensitive. This could have important implications for the CiPA initiative in terms of determining what temperature the step depolarisation protocol must be run at to acquire data that will be useful for constraining *in silico* models that will be used for simulations at physiological temperatures. In this regard, the CiPA High Throughput Stream (HTS), sponsored by the Health and Environmental Sciences institute (HESI), is about to embark on a large scale study using the step depolarisation protocol. As part of this study, data will be gathered describing kinetics and potency of hERG block using the step depolarisation protocol over multiple sites and platforms (including Patchliner, QPatch, CytoPatch, IonFlux and SyncroPatch) to assess the degree of data variability relative to the gold standard presented here. In addition, those sites with the capability will acquire data using the same platform at both ambient and physiological temperature in order to assess temperature dependence of kinetics and potency of hERG block using the step depolarisation protocol.

4.1.2 Drugs with fast binding kinetics

For over half of the drugs tested (ondansetron, ranolazine, sotalol, mexiletine, chlorpromazine, quinidine, diltiazem), the onset of block was too fast to measure using the step depolarisation protocol, but rather appeared to be instantaneous. In these cases, the true rate of block is as

fast, or faster than hERG activation at 0 mV (560 - 947 ms, Schuster *et al.*, 2011; Vandenberg *et al.*, 2006; Zhou *et al.*, 1998). This manifests as an apparent lack of concentration dependence to the timecourse of block since the time constant value measured (300 ms on average for all 7 drugs, see supplementary table 1 for values) does not actually reflect drug binding, but rather the rate limiting step is the rate of activation at 0 mV. Our measurement of the timecourse of block of the open channel, following ultrafast microfluidic exchange (Hill *et al.*, 2014; Windley *et al.*, 2016), are consistent with time constants of drug block that are indeed much faster than the rate of activation at 0 mV. The timecourse of block measured in this manner was also concentration dependent, contrary to the data obtained with the step depolarisation protocol. Both of these observations support the interpretation that the rate of channel opening is the limiting factor in measurement of the timecourse of block for fast drugs when using the step depolarisation protocol (Milnes *et al.*, 2010) at ambient temperature. We suggest that this limitation will also be the case for any protocol that requires pre-incubation of drug prior to measuring the onset of block as the channel activates. For drugs in this 'fast' category, block may simply have to be approximated as instantaneous when incorporated into *in silico* models for proarrhythmic risk prediction. It should be noted however, that while the direct application approach was informative in this context, it is not amenable to high-throughput testing since many current automated patch clamp systems do not have the capacity for such fast (<30 ms, Hill et al., 2014) solution switching.

4.1.3 Drug trapping

Using the step depolarisation protocol we were also able to obtain basic data on the relative degree of trapping observed for different drugs. Drug trapping occurs when drug does not fully dissociate from the channel following repolarisation (Mitcheson *et al.*, 2000). In this study the degree of trapping was measured as the proportion of the channel population that

remains drug bound between depolarizing steps (see Figure 7). However, using this dataset, it is not possible to determine to what degree this 'trapping' occurs as a result closure of the cytoplasmic gate to prevent diffusion of the drug molecule from the channel vestibule (Mitcheson *et al.*, 2000), slow dissociation from a high affinity open/inactivated state block or both (Lee *et al.*, 2016; Witchel *et al.*, 2004). It should also be noted that this measure of trapping is a snapshot imposed by the fixed 15 s interval at -80 mV between each depolarizing step. As a result, no information on the timecourse of recovery from trapping can be inferred below this threshold. For example, a drug that completely dissociated within 5 s could not be distinguished from one that dissociated in 15 s – they would both be classified as not trapped. Likewise, given a longer interval, drugs that remain trapped at 15 s may further dissociate. However, in the context of creating a model appropriate for the physiological conditions of the human heart, where a long beat-to-beat interval might be 2 s, such extreme periods at hyperpolarized membrane potentials are unlikely to occur.

Using this approach, the degree of trapping was measured as 18 %, 65 %, 79%, 97 % and 98 % for verapamil, cisapride, bepridil, terfenadine and dofetilide (Figure 7B). For 'fast' drugs (see section 4.1.2 above) we did not attempt to measure the degree of trapping since these compounds block effectively instantaneously, meaning steady state block is reached at the beginning of every sweep, regardless of whether trapping has occurred or not. The degree of trapping has previously been suggested to be associated with proarrhythmic risk (Di Veroli *et al.*, 2014), so it is interesting to note that all of the high-risk drugs that were tested showed a high degree of trapping. In this regard, this measure is being currently evaluated by the ISWG (Colatsky *et al.*, 2016) as a biophysical metric that may aid with *in silico* pro-arrhythmia risk prediction.

4.2 Comparison to Existing data

In general, the IC_{50} values for the twelve drugs, measured using the step depolarisation protocol corresponded well to those published within the literature. The observed discrepancies, where IC_{50}s were outside of the range of published IC_{50} values (chlorpromazine, bepridil and ranolazine, table 2), can likely be explained by the notable protocol dependency of hERG channel block (Kirsch *et al.*, 2004; Milnes *et al.*, 2010; Yao *et al.*, 2005). In regards to the timecourse of block, this is the first study to comprehensively assess drug binding kinetics for a diverse panel of drugs. Furthermore, only a few studies have directly measured the onset of block using the step depolarisation protocol described in this study, so limiting direct comparison. However, what information is available shows that the measured timecourse of block, like potency, is also very dependent on the protocol used to gather the data. For 10 nM cisapride for example, τ_{on} has been reported between 383 ms (Walker *et al.*, 1999) and 26 s (Windley *et al.*, 2016) compared to 42 s reported here. This variation demonstrates the importance of using a standardized protocol, such as that described here, to ensure consistency in the data describing the kinetics of hERG block that will be used to constrain the models to be used for *in silico* pro-arrhythmia risk prediction. An important next step will be to assess whether kinetics and potency measured for drug interactions with hERG 1a translate to I_{Kr}. While it might not be possible to acquire this dataset from native I_{Kr} in human cardiomyocytes, co-expression studies with hERG 1b and/or beta subunits in heterologous expression systems may go some way to answering this question.

4.3 Limitations.

One limitation of the protocol detailed in this study is the inability to measure the timecourse of drug washout. In principle, off rates for a simple bimolecular interaction can be calculated

from measurement of apparent on rates at multiple concentrations. However, this could be complicated by the complexities of state dependent drug binding (Ficker *et al.*, 1998; Perrin *et al.*, 2008) as well as the subtleties of the trapping phenomenon discussed above. It therefore remains to be seen how *in silico* approaches could overcome this issue. Secondly, the issue of temperature effects on kinetics of drug binding need to be considered. While this dataset is a benchmark for data gathered by most high throughput patch camp systems operating at ambient temperatures, more systems are now able to operate at physiological or near physiological temperatures (Obergrussberger *et al.*, 2015; Stoelzle *et al.*, 2011). Both potency (Kirsch *et al.*, 2004; Yao *et al.*, 2005) and kinetics (Windley *et al.*, 2016) of block have previously been shown to be temperature dependent. Managing these datasets acquired at diverse temperatures, and incorporating these temperature effects into *in silico* models will be an important short term focus for the field.

5. Conclusions

In this study, we describe the standardized implementation of the 'step depolarisation' protocol (Milnes et al, 2010) selected by the ICWG for measurement of kinetics and potency of hERG block for CiPA. The dataset assembled is the most comprehensive study of the kinetics of drug binding to hERG assembled to date and is freely available as the reference ambient temperature dataset to assess the variability in data acquired across high throughout automated platforms in industry. The dataset is currently being used by the *in silico* working group, together with parallel datasets acquired at physiological temperature, to develop *in silico* models of drug binding for use in risk prediction. This effort to accurately measure the kinetics of drug binding to hERG is motivated by the reasoning that this knowledge will help more accurately determine the risk profile of individual drugs. In a seminal paper, Campbell. (Campbell, 1983) subclassified Class I antiarrhythmics based on their kinetics and showed

this had practical consequences in determining refractoriness. Similarly, the kinetics of drugs interaction with hERG relative to both the kinetics of channel gating as well as the duration of the diastolic interval have been shown to be important in determining the degree of action potential prolongation and the emergence of proarrhythmic markers (Lee *et al.,* 2016). Indeed, it may eventuate that the grouping of hERG blocking drugs based on their kinetics may have some utility in future classification. The data presented in this study will provide the foundation to asses to what extent knowledge of drug binding kinetics can enhance our ability to assign risk, particularly through *in silico* approaches. We anticipate that further studies, extending the data to hERG 1a/1b expression and/or native I_{Kr} as well as investigating the effects of temperature will help further enhance the efficacy of these models in predicting risk.

Tables

Table 1: List of compounds, risk profile, and concentrations tested

Drug	Risk	Conc 1 (nM)/Fold free C_{max}	Conc 2 (nM)/Fold free C_{max}	Conc 3 (nM)/Fold free C_{max}
bepridil	High	10 / 0.3X	30 / 1X	100 / 3X
dofetilide	High	3 / 1.5X	10 / 5X	100 / 50X
quinidine	High	100 / 0.1X	300 / 0.3X	1000 / 1X
sotalol	High	30000 / 2X	100000 / 7X	300000 / 20X
chlorpromazine	Intermediate	100 / 3X	300 / 9X	1000 / 30X
cisapride	Intermediate	10 / 4X	30 / 12X	100 / 40X
ondansetron	Intermediate	300 / 1X	1000 / 3X	3000 / 10X
terfenadine	Intermediate	10 / 35X	100 / 350X	1000 / 3500X
diltiazem	Low	10000 / 100X	30000 / 300X	100000 / 1000X

mexiletine	Low	10000 / 4X	30000 / 12X	100000 / 40X
ranolazine	Low	10000 / 5X	30000 / 15X	100000 / 50X
verapamil	Low	100 / 2X	300 / 6X	1000 / 20X

Table 2: Comparison of IC_{50} values to the literature. (Data obtained from Crumb *et al.*, 2016; Hishigaki & Kuhara, 2011; Kirsch *et al.*, 2004; Kramer *et al.*, 2013; Redfern *et al.*, 2003, a, b, c, d and e, respectively)

Drug	IC_{50} (µM)	IC_{50} 95% CI	Hillslope	Hillslope 95% CI	IC_{50} comparison (µM)	IC_{50}/C_{max}	Literature IC_{50}/C_{max} (min – max)
bepridil	0.013	0.0096 – 0.017	1.1	0.7 – 1.6	0.023-0.149 [a, b, c, d, e]	0.4	0.7 – 55.7
dofetilide	0.0058	0.0044 – 0.0076	1.4	0.8 – 2.0	0.001-0.030 [a, b, d, e]	2.7	0.5 – 14.0
quinidine	0.235	0.202 – 0.274	1.3	1.0 – 1.5	0.3-1.1 [a, b, c, d, e]	0.3	0.4 – 1.3
sotalol	393	300 – 515	1.2	0.8 – 1.5	74-810 [a, c, d, e]	26.8	5.0 – 55.1
chlorpromazine	0.1663	0.146 – 0.190	1.4	1.1 -1.7	1.1-1.5 [a, d]	4.8	31.9 – 43.5
cisapride	0.0189	0.014 – 0.026	0.9	0.6 – 1.2	0.002-0.045 [a, b, c, d, e]	7.3	0.8 – 17.5
ondansetron	1.028	0.782 – 1.35	0.9	0.6 – 1.2	0.081-1.5 [a, b]	2.9	0.2 – 4.2
terfenadine	0.0131	0.012 – 0.014	1.0	0.9 – 1.1	0.0066-0.204 [a, b, c, d, e]	45.8	23.1 – 712.7
diltiazem	12.8	109 – 150	1.0	0.9 – 1.2	6.5-53.2 [a, d, e]	5981	3037 – 24 858
mexiletine	104.7	64.9 – 169	0.8	0.4 – 1.2	N/A	41.8	N/A
ranolazine	35.7	28.1 – 45.4	1.0	0.7 – 1.3	6.4-12 [a, e]	18.3	3.3 – 6.2
verapamil	0.3995	0.350 – 0.456	1.0	0.9 – 1.2	0.136-0.499 [a, b, c, d, e]	8.9	3.0 – 11.1

Figure legends

Figure 1: Depolarizing step protocol implementation. (A) hERG currents were recorded from CHO cells using whole cell patch clamp. Each experiment was divided into three phases: hERG currents were recorded in the absence of drug (i), drug was then applied to the closed channel at -80 mV (ii) and finally hERG currents were recorded in the presence of drug (iii). The timecourse of hERG block onset was assessed by using the offline subtraction routine illustrated in (B). Overlaid traces represent the last control sweep (I, black), the first hERG current response in the presence of drug (II, red) and the subtracted current (II-I, grey). The inset demonstrates the subtraction as a percentage of the control current (black) and the fitting of an exponential function to the data to calculate a time constant (τ) corresponding to the timecourse of block.

Figure 2: Representative leak corrected raw hERG data traces in response 10 s 0 mV voltage steps from a holding potential of -80 mV. The overlaid traces represent control (sweep 5, grey), the onset of drug block (sweep 11, coloured) and steady state block (sweeps 12-15).

Figure 3: Concentration response data for the CiPA training panel of 12 drugs. 3-4 concentrations were tested for each drug and data represents the mean $\pm$ SE of 4-5 cells. The percentage block was calculated from the current measured at the end of the 5th 0mV sweep in response to drug and expressed as a percentage of the current at the same time point of the last control sweep. Data was fit by Hill equation with the maxima and minima constrained to 100 and 0% respectively

Figure 4: Kinetics of hERG drug block. Plots represent the time constants for the onset of block (τ_{on}) for all drug concentrations where responses were successfully fit with an

exponential function. hERG currents were evoked by a 10s 0 mV voltage step from a holding potential -80mV. Data represents mean (black line) ± SE for n = 4-5, overlaid with the individual data points. Concentrations where the degree of block was too small to measure the timecourse of block accurately are marked (#).

Figure 5: Drugs where onset of block is too fast to accurately measure. (A) Shows a representative hERG trace where the onset of current was similar in the absence (black) and presence of 10, 30 and 100 μM diltiazem (green) in response to the 10 s 0mV voltage step from a holding potential of -80 mV. (B) Representative traces showing the direct application of 10, 30 and 100 μM diltiazem using a fast exchange system. hERG currents evoked at 0 mV were exposed to diltiazem for 20 s to measure the onset of block; the drug was washed out between applications. (C) Exponential functions used to measure the timecourse of drug block were fit to the raw direct application data (D) Values for the time constants were measured by fitting exponential functions to the onset of block for 10 s depolarizing step, subtracted protocols (closed circles) and direct application of drug via fast perfusion (open circles). Data represents the mean ± SE of 4-5 cells.

Figure 6: Drugs where onset of block is too slow to measure at 10 s. (A) shows a representative trace for 30 nM cisapride where the onset of block is too slow to measure accurately. The percentage block could be fit with a straight line. (B) Shows a comparison between time constants (τ_{on}) measured from 10, 20, 30 and 40 s duration 0mV voltage pulses. Data represents the mean ± the SD of 5 cells. (C) Representative traces of the 4 drugs with slow onset of block in response to 40 s 0mV voltage steps to 0mV from a holding potential of -80 mV at 15 s intervals. The control, the onset of block and subsequent sweeps are shown in black, dark colour and light colour, respectively. The time constants for all 4 slow drugs are

shown in (D). The data represents the mean ± SE and all data points are also shown. Closed circles indicate data obtained from 10s 0 mV voltage pulses and concentrations where the onset of block was too slow to measure are indicated by *.

Figure 7: Drug trapping. (A) Drug trapping was calculated from the percentage block data of the 1st drug sweep (red) in comparison to the percentage block at the beginning of the 5th drug sweep (black). Exponential curves were fit to the data and extrapolated back to t = 0 to calculate the difference between the first (red) and last (black) drug sweeps (i) and expressed as a fraction of steady state block (ii). (B) Comparison of calculated trapping values for drugs with τ_{on} values > 500 ms. Data represents mean ± SE of 4 cells and the measurements are overlaid.

Conflict of Interest

AH, BF, NA-G, JH and JV are members of the CiPA Ion Channel Working Group Rapid Response Team. BF and NA-G are co-chairs of the CiPA Ion Channel Working Group.

Funding

Acknowledgements

References

Aiba, T., Shimizu, W., Inagaki, M., Noda, T., Miyoshi, S., Ding, W. G., Zankov, D. P., Toyoda, F., Matsuura, H., Horie, M., & Sunagawa, K. (2005). Cellular and ionic mechanism for drug-induced long QT syndrome and effectiveness of verapamil. *J Am Coll Cardiol, 45*(2), 300-307.

Antzelevitch, C., Belardinelli, L., Zygmunt, A. C., Burashnikov, A., Di Diego, J. M., Fish, J. M., Cordeiro, J. M., & Thomas, G. (2004). Electrophysiological effects of ranolazine, a novel antianginal agent with antiarrhythmic properties. *Circulation, 110*(8), 904-910.

Barry, P. H. (1994). JPCalc, a software package for calculating liquid junction potential corrections in patch-clamp, intracellular, epithelial and bilayer measurements and for correcting junction potential measurements. *J Neurosci Methods, 51*(1), 107-116.

Campbell, T. J. (1983). Kinetics of onset of rate-dependent effects of Class I antiarrhythmic drugs are important in determining their effects on refractoriness in guinea-pig ventricle, and provide a theoretical basis for their subclassification. *Cardiovascular Research*, *17*(6), 344–352.

Carmeliet, E. (1992). Voltage- and time-dependent block of the delayed K+ current in cardiac myocytes by dofetilide. *Journal of Pharmacology and Experimental Therapeutics, 262*(2), 809-817.

Colatsky, T., Fermini, B., Gintant, G., Pierson, J. B., Sager, P., Sekino, Y., Strauss, D. G., & Stockbridge, N. (2016). The Comprehensive in Vitro Proarrhythmia Assay (CiPA) initiative - Update on progress. *J Pharmacol Toxicol Methods, 81*, 15-20.

Crumb, W. J., Jr., Vicente, J., Johannesen, L., & Strauss, D. G. (2016). An evaluation of 30 clinical drugs against the comprehensive in vitro proarrhythmia assay (CiPA) proposed ion channel panel. *J Pharmacol Toxicol Methods*.

Di Veroli, G. Y., Davies, M. R., Zhang, H., Abi-Gerges, N., & Boyett, M. R. (2014). hERG inhibitors with similar potency but different binding kinetics do not pose the same proarrhythmic risk: implications for drug safety assessment. *J Cardiovasc Electrophysiol, 25*(2), 197-207.

Fermini, B., Hancox, J. C., Abi-Gerges, N., Bridgland-Taylor, M., Chaudhary, K. W., Colatsky, T., Correll, K., Crumb, W., Damiano, B., Erdemli, G., Gintant, G., Imredy, J., Koerner, J., Kramer, J., Levesque, P., Li, Z., Lindqvist, A., Obejero-Paz, C. A., Rampe, D., Sawada, K., Strauss, D. G., & Vandenberg, J. I. (2016). A new perspective in the field of cardiac safety testing through the comprehensive in vitro proarrhythmia assay paradigm. *J Biomol Screen, 21*(1), 1-11.

Ficker, E., Jarolimek, W., Kiehn, J., Baumann, A., & Brown, A. M. (1998). Molecular determinants of dofetilide block of HERG K+ channels. *Circ Res, 82*(3), 386-395.

Gintant, G., Sager, P. T., & Stockbridge, N. (2016). Evolution of strategies to improve preclinical cardiac safety testing. *Nature Reviews Drug Discovery, 15*(7), 457-471.

Gualdani, R., Tadini-Buoninsegni, F., Roselli, M., Defrenza, I., Contino, M., Colabufo, N. A., & Lentini, G. (2015). Inhibition of hERG potassium channel by the antiarrhythmic agent mexiletine and its metabolite m-hydroxymexiletine. *Pharmacology Research and Perspectives, 3*(5), e00160.

Hancox, J. C., McPate, M. J., El Harchi, A., & Zhang, Y. H. (2008). The hERG potassium channel and hERG screening for drug-induced torsades de pointes. *Pharmacology and Therapeutics, 119*(2), 118-132.

Hill, A. P., Perrin, M. J., Heide, J., Campbell, T. J., Mann, S. A., & Vandenberg, J. I. (2014). Kinetics of drug interaction with the Kv11.1 potassium channel. *Mol Pharmacol, 85*(5), 769-776.

Hishigaki, H., & Kuhara, S. (2011). hERGAPDbase: a database documenting hERG channel inhibitory potentials and APD-prolongation activities of chemical compounds. *Database (Oxford)*, bar017.

Kirsch, G. E., Trepakova, E. S., Brimecombe, J. C., Sidach, S. S., Erickson, H. D., Kochan, M. C., Shyjka, L. M., Lacerda, A. E., & Brown, A. M. (2004). Variability in the measurement of hERG potassium channel inhibition: effects of temperature and stimulus pattern. *J Pharmacol Toxicol Methods, 50*(2), 93-101.

Kramer, J., Obejero-Paz, C. A., Myatt, G., Kuryshev, Y. A., Bruening-Wright, A., Verducci, J. S., & Brown, A. M. (2013). MICE models: superior to the HERG model in predicting Torsade de Pointes. *Sci Rep, 3*, 2100.

Lee, W., Mann, S. A., Windley, M. J., Imtiaz, M. S., Vandenberg, J. I., & Hill, A. P. (2016). In silico assessment of kinetics and state dependent binding properties of drugs causing acquired LQTS *Progress in Biophysics & Molecular Biology, 120*(1-3), 89-99.

Li, Z., Dutta, S., Sheng, J., Tran, P. N., Wu, W., & Colatsky, T. (2016). A temperature-dependent in silico model of the human ether-a-go-go-related (hERG) gene channel. *J Pharmacol Toxicol Methods, 81*, 233-239.

Milnes, J. T., Witchel, H. J., Leaney, J. L., Leishman, D. J., & Hancox, J. C. (2010). Investigating dynamic protocol-dependence of hERG potassium channel inhibition at 37 degrees C: Cisapride versus dofetilide. *J Pharmacol Toxicol Methods, 61*(2), 178-191.

Mitcheson, J. S., Chen, J., & Sanguinetti, M. C. (2000). Trapping of a methanesulfonanilide by closure of the HERG potassium channel activation gate. *J Gen Physiol, 115*(3), 229-240.

Obergrussberger, A., Stolzle-Feix, S., Becker, N., Bruggemann, A., Fertig, N., & Moller, C. (2015). Novel screening techniques for ion channel targeting drugs. *Channels (Austin), 9*(6), 367-375.

Perrin, M. J., Kuchel, P. W., Campbell, T. J., & Vandenberg, J. I. (2008). Drug binding to the inactivated state is necessary but not sufficient for high-affinity binding to human ether-a-go-go-related gene channels. *Mol Pharmacol, 74*(5), 1443-1452.

Redfern, W. S., Carlsson, L., Davis, A. S., Lynch, W. G., MacKenzie, I., Palethorpe, S., Siegl, P. K., Strang, I., Sullivan, A. T., Wallis, R., Camm, A. J., & Hammond, T. G. (2003). Relationships between preclinical cardiac electrophysiology, clinical QT interval prolongation and torsade de pointes for a broad range of drugs: evidence for a provisional safety margin in drug development. *Cardiovasc Res, 58*(1), 32-45.

Roden, D. M. (2004). Drug-induced prolongation of the QT interval. *The New England Journal of Medicine, 350*(10), 1013-1022.

Sager, P. T., Gintant, G., Turner, J. R., Pettit, S., & Stockbridge, N. (2014). Rechanneling the cardiac proarrhythmia safety paradigm: a meeting report from the Cardiac Safety Research Consortium. *American Heart Journal, 167*(3), 292-300.

Schuster, A. M., Glassmeier, G., & Bauer, C. K. (2011). Strong activation of ether-a-go-go-related gene 1 K+ channel isoforms by NS1643 in human embryonic kidney 293 and Chinese hamster ovary cells. *Mol Pharmacol, 80*(5), 930-942.

Shah, R. R. (2008). Drug-induced QT interval prolongation—regulatory guidance and perspectives on hERG channel studies *The hERG cardiac potassium channel: structure, function and long QT syndrome* (pp. 251-285): John Wiley & Sons, Ltd.

Spector, P. S., Curran, M. E., Keating, M. T., & Sanguinetti, M. C. (1996). Class III antiarrhythmic drugs block HERG, a human cardiac delayed rectifier K+ channel. Open-channel block by methanesulfonanilides. *Circ Res, 78*(3), 499-503.

Stoelzle, S., Obergrussberger, A., Bruggemann, A., Haarmann, C., George, M., Kettenhofen, R., & Fertig, N. (2011). State-of-the-art automated patch clamp devices: heat activation, action potentials, and high throughput in ion channel screening. *Front Pharmacol, 2*, 76.

Vandenberg, J. I., Varghese, A., Lu, Y., Bursill, J. A., Mahaut-Smith, M. P., & Huang, C. L. (2006). Temperature dependence of human ether-a-go-go-related gene K+ currents. *American Journal of Physiology - Cell Physiology, 291*(1), C165-175.

Walker, B. D., Singleton, C. B., Bursill, J. A., Wyse, K. R., Valenzuela, S. M., Qiu, M. R., Breit, S. N., & Campbell, T. J. (1999). Inhibition of the human ether-a-go-go-related gene (HERG) potassium channel by cisapride: affinity for open and inactivated states. *Br J Pharmacol, 128*(2), 444-450.

Windley, M. J., Mann, S. A., Vandenberg, J. I., & Hill, A. P. (2016). Temperature effects on kinetics of KV11.1 drug block have important consequences for in silico proarrhythmic risk prediction. *Mol Pharmacol, 90*(1), 1-11.

Witchel, H. J., Dempsey, C. E., Sessions, R. B., Perry, M., Milnes, J. T., Hancox, J. C., & Mitcheson, J. S. (2004). The low-potency, voltage-dependent HERG blocker propafenone--molecular determinants and drug trapping. *Mol Pharmacol, 66*(5), 1201-1212.

Yao, J. A., Du, X., Lu, D., Baker, R. L., Daharsh, E., & Atterson, P. (2005). Estimation of potency of HERG channel blockers: impact of voltage protocol and temperature. *J Pharmacol Toxicol Methods, 52*(1), 146-153.

Zhou, Z., Gong, Q., Ye, B., Fan, Z., Makielski, J. C., Robertson, G. A., & January, C. T. (1998). Properties of HERG channels stably expressed in HEK 293 cells studied at physiological temperature. *Biophys J, 74*(1), 230-241.
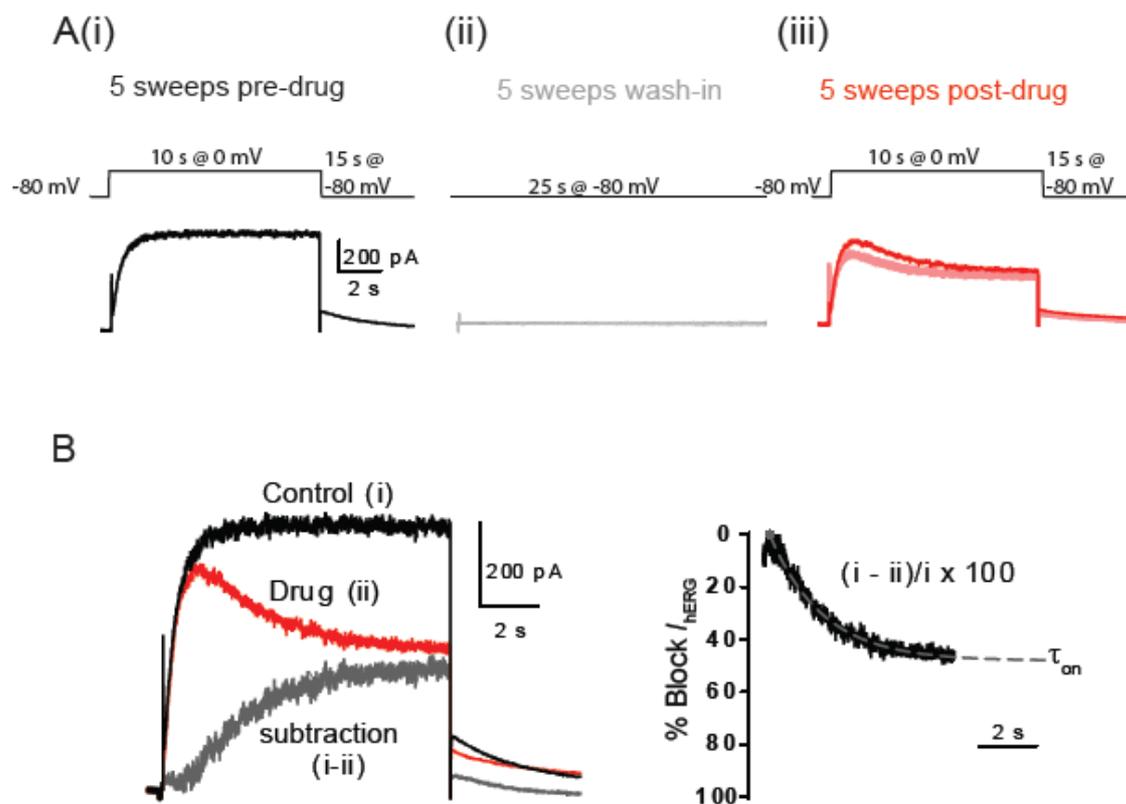
Fig. 1

A(i) 5 sweeps pre-drug

(ii) 5 sweeps wash-in

(iii) 5 sweeps post-drug

-80 mV | 10 s @ 0 mV | 15 s @ -80 mV

25 s @ -80 mV | -80 mV

-80 mV | 10 s @ 0 mV | 15 s @ -80 mV

200 pA
2 s

B

Control (i)

Drug (ii)

subtraction (i-ii)

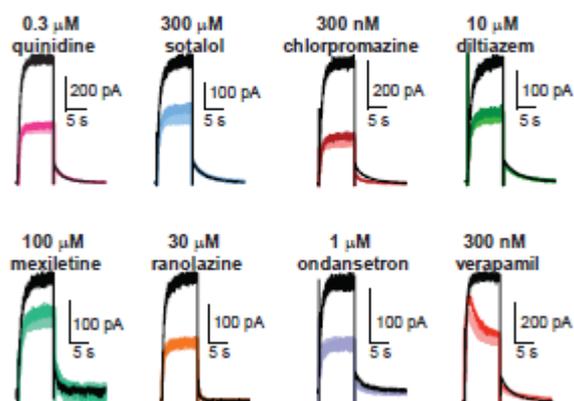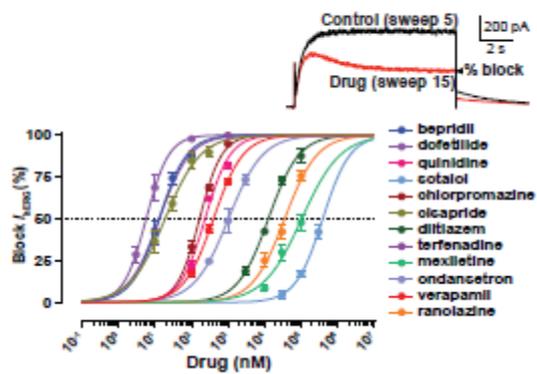200 pA
2 s

% Block I_{hERG}

0
20
40
60
80
100

(i – ii)/i x 100

τ_{on}

2 s

Fig. 2

Fig. 3

Fig. 4

Fig. 5

Fig. 6

A

control

30 nM
cisapride

subtraction

200 pA
2 s

I_{hERG} block (%)

τ_on

2 s

B

τ_on (s)

	10 s	20 s	30 s	40 s
	13203	206.2	31.4	26
	23981	392.6	14.3	6.9

Sweep duration (s)

C

10 nM dofetilide

100 pA
5 s

10 nM terfenadine

100 pA
5 s

30 nM cisapride

200 pA
5 s

10 nM bepridil

100 pA
5 s

D

τ_on (s)

bepridil   dofetilide   cisapride   terfenadine

Drug (nM)

Fig. 7